OHCs SHIFT THE EXCITATION PATTERN VIA BM TENSION

J.B. ALLEN
AT&T Research Laboratory,
Murray Hill, NJ 07974,
jba@research.att.com

We now know that outer hair cells (OHC) nonlinearly compress the dynamic range of basilar membrane motion [26,27] and the neural response,[31] extending the otherwise limited dynamic range of the inner hair cell (IHC) response.[21,2] This role of the OHC may be quantified using many objective measures. *Loudness*, measured by Fletcher and Munson's [18] loudness balance method, shows a 1/3 power law compressive function of intensity (i.e., Stevens' Law). This dynamic loudness compression is provided by normal OHC function.[7] *Recruitment* results when there is loss of this compression, as when OHCs are damaged.[29,10,2,3,4] *Masking patterns* provide a psychoacoustic measure of cochlear nonlinearity. The OHC compression show up in the 1923–1924 masking growth curves of Fletcher [14] and Wegel and Lane [30] as the *upward spread of masking*. The elevated tails of tuning curves are also evident in the upward spread of masking data as the elevated threshold. These masking data also seem very similar to *two–tone suppression* results.[1,13] Otoacoustic emissions (*SFOAEs* and *DPOAEs*) are an objective measure of the OHC nonlinear compression.[9] I shall connect these physical and psychoacoustic measures using a cochlear model whose basilar membrane (BM) stiffness is signal dependent as a result of a dynamic change in BM radial tension by the outer hair cells.[20] According to this nonlinear model, as the signal intensity increases, the BM radial tension decreases, resulting in a decreased local BM stiffness, and therefore a basal shift of the BM and neural excitation patterns (EP) by up to $\approx$1/2 octave.[6] This EP shift shows up in basilar membrane velocity data, cochlear microphonics, neural "revcor" functions, simultaneous and forward masking patterns, two–tone suppression data, and noise trauma studies. When the steep apical (low–pass) slope of the low–loss BM traveling wave shifts across the basal (high–pass) response of the tectorial membrane transfer function,[5,6,8] a narrow–band neural–like compressed tuning results. The resulting CF sensitivity is compressive, with a power–bandwidth (ERB) that is approximately independent of intensity, consistent with the *critical ratio* measure of Fletcher (1938), Egan and Hake (1950),[16,17,12,4] as well as some more recent animal data. Thus OHCs play an important and quantifiable role in loudness, neurosensory hearing loss, masking, two–tone suppression, and OAEs.

1 Introduction

Our understanding of the auditory system's large 120 dB dynamic range is fundamentally incomplete. For example, *recruitment*, the most common form of neurosensory hearing loss, is best characterized as the loss of dynamic range.[29,3,4] Recruitment results from outer hair cell damage.[10] To successfully design hearing aids that deal with the problem of recruitment, we need models that improve our understanding of *how* the cochlea achieves this dynamic range.

I shall begin by showing that the dynamic range of the IHC must be less than 65 dB (in fact it is probably less than 50 dB, but I can not prove this). This raises the question: *How can the basic cochlear detectors (the IHCs) have a dynamic range of less than 65 dB, and yet the auditory system has a dynamic range of 120 dB?* A great deal of indirect evidence shows that this extra dynamic range results from mechanical nonlinear signal compression provided by outer hair cells. This compression

shows up in auditory psychophysics and in cochlear physiology in many ways. In this paper we summarize some of the basic relationships between the OHC and various psychophysical measures to explore *how* OHCs extend the IHC dynamic range.

2 The Dynamic Range Problem

The question of dynamic range in the auditory system is a long standing problem. Previously this question has been raised in the context of both the nerve cell and the synapse. I am raising the same question, but presynaptically, with respect to the IHC's transmembrane voltage, which is limited at the high end by the open circuit voltage seen by the cell, and at the low end by the membrane Johnson noise and cilia Brownian motion.

It is argued here that the main function of the OHCs is to solve this cochlear dynamic range problem. This argument consists of showing that the inner hair cell transmembrane voltage dynamic range (i.e., the cell's functional range) is less than 65 dB. From estimates of (a) the RMS Johnson (thermal) noise voltage, and (b) the maximum available signal voltage across the hair cell membrane, we may bound the IHC transmembrane voltage dynamic range. If the dynamic range in acoustic intensity is greater than the dynamic range of the IHC detectors, one must conclude that the signal driving the IHC detectors is compressed. Many studies have identified the OHC as the source of the this compression, starting with the speculations of Lorente de No in 1937 [22] following the discovery of loudness recruitment.

The RMS transmembrane thermal Johnson noise voltage V_c of the IHC is given by

$$V_c^2 = 2kTR\int_{-\infty}^{\infty}\frac{1}{1+(2\pi fRC)^2}df = \frac{kT}{C}. \qquad (1)$$

where R is the membrane leakage resistance and C the membrane capacitance. The IHC capacitance has been found to be about 9.6 pF by Kros and Crawford.[19] From Eq. 1, V_c = 21.1 μV RMS at body temperature (k = 1.38$\times$10^{-23} Joule/degree-Kelvin, T = 310° K).

The maximum open circuit DC voltage across the cilia is about 120 mV. The maximum change in cell voltage that has been observed is 30 mV RMS (Russell, personal communication). The ratio of 30 mV to the noise floor voltage (e.g., 21.1 μV), expressed in dB, is 63 dB. The maximum dynamic range in signal intensity of the auditory system is approximately 120 dB. This leaves about 57 dB of dynamic range unexplained. We conclude that *there must be nonlinear compression (level dependent gain) built into the mechanics of the cochlea* to account for the large acoustic dynamic range. Since the discovery of loudness recruitment it has been suspected that it is the job of the OHCs to provide this compression.[22,10] The real question before us is: *What is the chain of events that leads to the stimulus compression seen by the IHCs?*

Estimate of the Cilia Displacement at the Hearing Threshold. Russell *et al.* have estimated the *in vitro* sensitivity of the mouse culture hair cell as 0.4 mV/nm, or 30 mV/degree of angular rotation of stereo cilia.[28] Assuming a thermal noise floor of 20

Table 1: Estimates of various cochlear measures at 0, 60, and 120 dB SPL at 1 kHz. The BM displacement data is from Nuttall[25] and is at 18 kHz. Column "SLOPE (dB)" shows the dB ratio of the dynamic range of the "MEASURE" to the dynamic range of the sound intensity.

MEASURE (UNITS)	THRESHOLD	—	MAXIMUM	SLOPE (dB)
Power (Watts/cm^2)	10^{-16}	10^{-10}	10^{-4}	
Intensity (dB-SPL)	0	60	120	
Stapes displacement (nm)	0.001	1	1000	1
BM displacement (nm)	0.2	7	?	0.61
Cilia displacement (nm)	0.05	1.1	$<$50 (1°)	0.5
IHC voltage (mV)	0.02	0.67	30	0.53

μV RMS, the IHC displacement sensitivity of the cell at the thermal-noise threshold is 0.05 nm. Given that 1 degree of cilia displacement corresponds to 30 mV, a cilia displacement of more than a degree would drive the cell into saturation, and would likely rupture the delicate structures of the cilia transduction channels. A summary of dynamic level estimates of the stapes, basilar membrane, cilia displacements, and IHC RMS voltage levels, is provided in Table 1.

The conclusion that the OHCs must be compressing the dynamic range of the IHC's excitation signal (e.g., the TM–RL shear) is further supported by basilar membrane velocity measurements which show a nonlinear growth of response. However there are several problems. While the BM data show compression, this compression is different in many ways from that of the IHC excitation signal. For example, recent two–tone BM suppression results have been found to be quite different from the corresponding neural measures.[11] Furthermore the bandwidth (ERB) of the BM signal is not in agreement with detection experiments of tones in wide band noise, namely critical ratio experiments of Fletcher and others. In this paper we shall explore old psychophysical data with new insights.

3 Tone–on–Tone Masking

In 1923 Fletcher[14] and 1924 Wegel and Lane[30] described the first detailed *narrow–band* tone masker, tone maskee (*tone–on–tone masking*) simultaneous masking data for masker frequencies f_m between 0.25 and 4 kHz and intensities between 0 and 85 dB SL. These data provided a very basic measure of the hearing process that, while frequently verified, is not understood to this day. When we explain these masking data, we will better understand the role of the OHC compression. Figure 1 shows *masking level curves* $M(f_p, f_m, I_m)$ for a f_m = 400 Hz masker, with f_p as the parameter. The masking is defined as $M \equiv I_p^*/I_{\text{ref}}$. The $*$ on I_p^* indicates that I_p is at the detection threshold. The intensity $I_{\text{ref}} = I_p^*$ is the threshold intensity of the probe when the masker is off (I_m = 0). These data follow a power–law intensity dependence

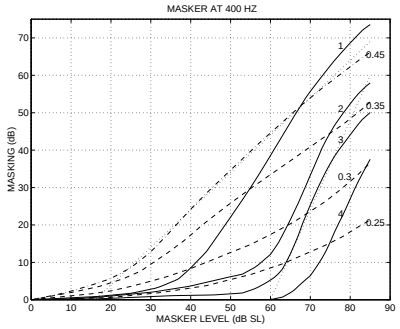

Figure 1: Tone–masking–tone data from Fletcher (1923) and Wegel and Lane (1924) for a masker at 400 Hz. The dashed lines correspond to probe frequencies between 0.25–0.45 kHz, while the solid lines correspond to probe frequencies of 1–4 kHz. The masking between 0.4 and 0.45 kHz is proportional to the masker level (i.e., the slope is close to 1). For 2, 3, and 4 kHz there is a threshold effect between 55–65 dB SL. For these frequencies the slope is greater than 1. For probe frequencies below the masker the slopes change with level, but is always less than 1.

of the threshold probe intensity on the masker intensity, namely

$$\frac{I_p^*}{I_{\text{ref}}} = \left(\beta \frac{I_m}{I_{\text{ref}}}\right)^{\kappa}, \tag{2}$$

with an exponent κ that systematically depends on the relative frequency between the masker and the probe. There are three basic regions of masking patterns corresponding to *critical–band masking* ($f_p \approx f_m$), the *downward spread of masking* ($f_p < f_m$), and the *upward spread of masking* ($f_p > f_m$). For probes higher in frequency than the masker frequency, the exponent κ is much greater than 1. For probes lower in frequency than the masker frequency, the exponent is less than 1. When the probe and masker are within the critical band, the exponent is close to 1.

Critical–Band Masking. For probe frequencies near the masker frequency of 400 Hz the masking is approximately characterized as *linear in intensity*.[30] For example, at f_p = 0.45 kHz (dash-dot line in Fig. 1) the masking curve is well approximated by the linear relation (κ = 1, β = 1/40)

$$\frac{I_p^*(f_p, I_m)}{I_m} = \frac{1}{40} \tag{3}$$

for I_m greater than about 25 dB SL, as indicated by the dotted line superimposed on the 0.45 kHz masking curve. Equation 3 is similar to Weber's Law for JNDs, extended to the case of masking (i.e., $\Delta I \equiv I_p^*$).

While the "linearity of masking" seems to be a trivial empirical observation, it is a surprising result. It is not obvious, at first glance, why the masking should be proportional to intensity. When the probe is added to the masker within a critical–bandwidth, the basilar membrane motion signals add (e.g., two sin waves beat). However, the re-

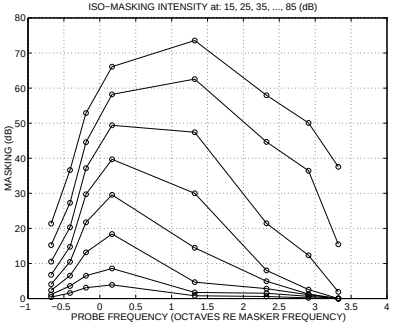

Figure 2: When the data of Fig. 1 is plotted as masking patterns, we see the upward spread of masking as well as the 1/2 octave shift in the frequency of greatest masking.

sponse level of the basilar membrane motion, the neural response, and the resulting loudness are all compressive–nonlinear functions of level. In fact the observation summarized by Eq. 3 inspired the famous JND experiments of Riesz (1928) which were the first to show that, for tones, the exponent is not exactly 1 (the "near miss" to Weber's law).

Below about 60 dB-SL the masking is greatest near the masker frequency. At 67 dB-SL the masking curve corresponding to the 1000 Hz probe frequency crosses the 450 Hz curve, as the frequency of maximum masking shifts to higher frequencies. At 80 dB–SL the probe frequency corresponding to the maximum masking is about 1.5 octaves above the masker frequency. This is more easily seen in Fig. 2 where the data of Fig. 1 have been plotted as iso-intensity contours (i.e., *masking patterns*).

We conclude that *the excitation pattern (EP) shifts toward the base as the intensity is raised.* Based on model studies, the most likely explanation for the EP shift is a BM stiffness change with level.[6,5] These studies showed that the IHC compressive nonlinearity can be also be explained by a dynamic BM stiffness, assuming the tectorial membrane acts as a high–pass filter. We extend this model by adding LePage's assumption that the dynamic radial BM tension controls the BM stiffness,[20] due to a signal dependent dynamic OHC stiffness or length change.

The Spread of Masking. As may be seen from Fig. 1 (solid lines) for the *upward spread of masking* case (f_p = 2–4 kHz $> f_m$), the onset of masking is abrupt at about 55–65 dB ($\beta = 10^{-6}$) and has a slope (on log–log scales) of κ = 2.4, that is

$$\frac{I_p^*(f_p, I_m)}{I_{\text{ref}}} = \left(10^{-6}\frac{I_m}{I_{\text{ref}}}\right)^{2.4}.$$

This expression is shown in Fig. 1 as the dotted line, superimposed on the 3 kHz probe curve. This steep slope is loosely referred to as the *upward spread of masking*. The expansive power–law exponent of κ = 2.4 must depend on the the basilar membrane

compression at the masker frequency, independent of the probe frequency f_p, because the high frequency probe excites the basal "tail" region of the EP where the basilar membrane response is approximately linear. It logically follows that the exponent $\kappa = 2.4$ must be the reciprocal of the basilar membrane compression exponent ($0.42 \approx 1/2.4$) at the masking frequency's characteristic place.

For the *downward spread of masking* case ($f_p < f_m$) (dashed lines), the growth of masking is a compressive power law ($\kappa < 1$) with an exponent κ that depends on intensity as well as probe frequency. In this case there is no clear "threshold" effect, as there is in the $f_p > f_m$ case. For this case Eq. 2 is not as useful a representation since κ depends on all the variables. The amount of masking depends on the steep apical slope of the masker excitation pattern and its spreading into the region of the probe. From Fig. 1, as the masker level is raised, the masking is less than would be predicted by a linear (κ = 1) growth of masking. From Fig. 2, as the intensity of the masker is increased, the masker excitation pattern shifts away from the low intensity probe masking pattern, reducing the relative masking. As the probe intensity reaches higher levels, its masking pattern also begins to shift toward the base, leading asymptotically to a linear growth of masking at higher levels.

Forward Masking and Two–Tone Suppression. The shift in the excitation pattern is confounded by the fact that both the probe and masker are on simultaneously. Is the basal shift in the EP still seen at high levels for forward masking? The answer to this is yes, as was first shown by Munson and Gardner in 1950,[24] and later by Lutfi.[23] Data from these papers clearly show that the 1/2 octave shift in the EP does not depend on the probe and masker being present simultaneously and provide data that may allow us to estimate the release time of the BM stiffness change.

Two–tone suppression has many properties in common with the masking data of Fig. 1. For example, when the suppressor is *higher* in frequency than the suppressed (CF) probe, the suppression growth is shallow (i.e., weak), and is present at low levels. This case is similar to the low frequency probes of Fig. 1. When the suppressor is *lower* in frequency, the suppression growth is steep (i.e., strong) and has a threshold at about 55-65 dB SPL.[13,1] It seems that the explanation given in this paper for masking also applies to two–tone suppression.

Summary. It appears that cochlear compression and the shifting excitation pattern are both related to normal OHC function. To shift the EP, the OHC stiffness or length change must change the BM stiffness. If the BM stiffness is determined by the radial tension in the BM, as proposed by Fletcher,[15] and LePage,[20] then a local change in the BM tension would change the local BM stiffness, and therefore the BM tuning.[6] This would result in a shift of the excitation patterns with intensity, as observed in the masking pattern data.

References

1. P. Abbas and M. Sachs. Two–tone suppression in auditory–nerve fibers: Extension of a stimulus–response relationship. *Journal of the Acoustical Society of America*, 59(1):112–122, Jan. 1976.

2. J. Allen. DeRecruitment by multiband compression in hearing aids. In W. Jesteadt and *et al.*, editors, *Modeling Sensorineural Hearing Loss*. Lawrence Erlbaum, Inc., Hillsdale, NJ, 1996.
3. J. Allen. DeRecruitment by multiband compression in hearing aids. In B. Kollmeier, editor, *Psychoacoustics, speech, and hearing aids*. World Scientific, Singapore, 1996.
4. J. Allen. Harvey Fletcher's role in the creation of communication acoustics. *Journal of the Acoustical Society of America*, 99(4):1825–1839, Apr. 1996. Reprint of material from preface of Fletcher's 53 book, with some important additions on the critical band.
5. J. B. Allen. Cochlear micromechanics: A physical model of transduction. *Journal of the Acoustical Society of America*, 68(6):1660–1670, 1980.
6. J. B. Allen. Modeling the noise damaged cochlea. In P. Dallos, C. D. Geisler, J. W. Matthews, M. A. Ruggero, and C. R. Steele, editors, *The Mechanics and Biophysics of Hearing*, pages 324–332, New York, 1990. Springer-Verlag.
7. J. B. Allen. Harvey Fletcher 1884–1981. In J. B. Allen, editor, *The ASA edition of* Speech, Hearing in Communication. Acoustical Society of America, Woodbury, New York, 1995.
8. J. B. Allen and P. F. Fahey. A second cochlear-frequency map that correlates distortion product, neural tuning measurements. *J. Acoust. Soc. Am.*, 94(2, Pt. 1):809–816, Aug. 1993.
9. J. B. Allen and B. L. Lonsbury-Martin. Otoacoustic emissions. *Journal of the Acoustical Society of America*, 93(1):568–569, Jan. 1993.
10. W. F. Carver. Loudness balance proceedures. In J. Katz, editor, *Handbook of clinical audiolgy, 2^d edition*, chapter 15, pages 164–178. Williams and Wilkins, Baltimore MD, 1978.
11. N. Copper and W. Rhode. Two tone suppression and two tone distortion in apical and basal cochlear mechanics. In *The Nineteenth ARO midwinter meeting*, number 220 in 19, page 55, Feb. 1996.
12. J. Egan and H. Hake. On the masking pattern of a simple auditory stimulus. *Journal of the Acoustical Society of America*, 22:662–630, 1950.
13. P. F. Fahey and J. B. Allen. Nonlinear phenomena as observed in the ear canal, at the auditory nerve. *Journal of the Acoustical Society of America*, pages 599–612, Feb. 1985.
14. H. Fletcher. Physical measurements of audition and their bearing on the theory of hearing. *Journal of the Franklin Institute*, 196(3):289–326, Sept. 1923.
15. H. Fletcher. A space-time pattern theory of hearing. *Journal of the Acoustical Society of America*, 1:311–343, Apr. 1930.
16. H. Fletcher. Loudness, masking and their relation to the hearing process and the problem of noise measurement. *Journal of the Acoustical Society of America*, 9:275–293, Apr. 1938.
17. H. Fletcher. The mechanism of hearing as revealed through experiments on the masking effect of thermal noise. *Proceedings National Academy Science*, 24:265–274, 1938.
18. H. Fletcher and W. Munson. Loudness, its definition, measurement, and calculation. *Journal of the Acoustical Society of America*, 5:82–108, 1933.
19. C. Kros and A. Crawford. Potassium currents in inner hair cells isolated from the guinea–pig cochlea. *Journal of Physiology*, 421:263–291, 1990.
20. E. LePage. Helmholtz revisited: Direct mechanical data suggest a physical model for dynamic control of mapping frequency to place along the cochlear partition. In P. Dallos, C. D. Geisler, J. W. Matthews, M. A. Ruggero, and C. R. Steele, editors, *The Mechanics and Biophysics of Hearing*, pages 278–287, New York, 1990. Springer-Verlag.
21. M. Liberman. Single-neuron labeling and chronic cochlear pathology III. Stereocilia damage and alterations of tuning curve thresholds. *Hearing Research*, 16:55–74, 1984.
22. R. Lorente de No. The diagnosis of diseases of the neural mechanism of hearing by the aid of sounds well above threshold. *Trans. Am. Otol. Soc.*, 27:219–220, 1937. Discussion of E. P. Fowler's paper on recruitment.
23. R. Lutfi. Complex interactions between pairs of forward maskers. *Hearing Research*, 35:71–78, 1988.
24. W. Munson and M. Gardner. Loudness patterns – a new approach. *Journal of the Acoustical Society of America*, 22(2):177–190, Mar. 1950.
25. A. Nuttall and D. Dolan. Steady–state sinusoidal velocity responses of the basilar membrane in guinea pig. *Journal of the Acoustical Society of America*, 99(3):1556–1565, Mar. 1996.
26. W. Rhode. Observations of the vibration of the basilar membrane in squirrel monkeys using the Mössbauer technique. *Journal of the Acoustical Society of America*, 49, 1971.
27. M. Ruggero, L. Robles, and N. Rich. Middle-ear response in the chinchilla and its relationship to mechanics at the base of the cochlea. *Journal of the Acoustical Society of America*, 87:1612–1629, 1990.
28. I. Russell, Richardson, and Cody. Mechanosensitivity of mammalian auditory hair cells *in vitro*. *Nature*, 321(29):517–519, May 1986.
29. J. Steinberg and M. Gardner. Dependence of hearing impairment on sound intensity. *Journal of the Acoustical Society of America*, 9:11–23, July 1937.
30. R. Wegel and C. Lane. The auditory masking of one pure tone by another and its probable relation to the dynamics of the inner ear. *Physical Review*, 23:266–285, Feb. 1924.
31. G. Yates, I. Winter, and D. Robertson. Basilar membrane nonlinearity determines auditory nerve rate–intensity functions and cochlear dynamic range. *Hearing Research*, 45:203–220, 1989.